IEEE Access
Multidisciplinary | Rapid Review | Open Access Journal

Received February 2, 2019, accepted February 28, 2019, date of publication March 7, 2019, date of current version March 25, 2019.

Digital Object Identifier 10.1109/ACCESS.2019.2903438

Compact and Low-Loss V-Band Waveguide Phase Shifter Based on Glide-Symmetric Pin Configuration

ANGEL PALOMARES-CABALLERO[1], ANTONIO ALEX-AMOR[1], PABLO PADILLA[2], FRANCISCO LUNA[1], AND JUAN VALENZUELA-VALDES[2]

[1]Departamento de Lenguajes y Ciencias de la Información, Universidad de Málaga, 29071 Málaga, Spain
[2]Departamento de Teoría de la Señal, Telematica y Comunicaciones, Universidad de Granada, 18071 Granada, Spain

Corresponding author: Angel Palomares-Caballero (angelpc@uma.es)

This work was supported in part by the Spanish Research and Development National Program and FEDER under project TIN2016-75097-P, in part by the Universidad de Málaga, under Grant PPIT.UMA.B1.2017/15, in part by the Universidad de Granada under Project PPJI2017.15, and in part by the Universidad de Granada through the grant program "Becas de iniciación a la investigación" from the Plan Propio de Investigación.

ABSTRACT This paper presents a compact and low-loss V-band waveguide phase shifter based on glide-symmetric pin configuration. This kind of higher symmetry permits the control and improvement of the electromagnetic behavior or radiofrequency devices, as it is the case of the proposed phase shifter. The study of the dispersion diagram of the phase shifter unitary cell demonstrates that the pin configuration is a proper option for introducing a phase shift in a waveguide-based system. There is a significant increase in terms of phase shift when using a glide-symmetric pin distribution compared to its corresponding non-glide-symmetric configuration. Through this paper, the key geometrical parameters are also determined. The complete phase shifter is composed of an optimized cascade of tailored unitary cells so that the desired final phase shift value is achieved. A prototype has been manufactured in order to validate the theoretical approach through the comparison of phased shifters with both non-glide-symmetric and glide-symmetric configurations. The measurement results demonstrate the higher performance and compactness of the glide-symmetric phase shifter. For the same distance, the glide-symmetric version of the phase shifter provides more than 60% of phase shifting compared to the non-glide-symmetric phase shifter. Both phase shifters have a good impedance matching between 46 and 60 GHz and an insertion loss lower than 1 dB, thus clearly enabled as a 5G technology.

INDEX TERMS Phase shifter, millimeter-wave, glide symmetry, gap waveguide.

I. INTRODUCTION

Digital society is evolving faster and faster and new applications are being created that demand unprecedented performance from mobile communications, some of which are expected to require communication speeds of the order of Terabit/s. To satisfy these requirements, it is necessary to develop high data transfer communication systems allowing these speeds, which makes it is essential to perform communications in a frequency band above 50 GHz. Traditional radiofrequency solutions do not work for this frequency bands and new technologies have to be developed. In the first place it is necessary to develop very directive antennas to face the propagation losses that exist at those frequencies. In that way, beamforming is one of the major goals of the future generation of communication systems. The steering of the radiated beam in wireless communication links is possible by means of antenna arrays whose input signals are controlled in amplitude and phase. Beamforming networks [1]–[3] are typically used for this purpose. Millimeter-wave range is a challenging spectrum range in these next-generation systems. In this frequency ranges, the beamforming networks are needed for producing directive beams that overcome the undesired effect of the high propagation losses in this frequency range [4]–[7].

Beamforming networks make use of phase shifters that provide a different amount of phase shift depending on the requirements. These phase shifters need to be lossless and

The associate editor coordinating the review of this manuscript and approving it for publication was Feng Lin.

compact in order to achieve the maximum efficiency and reduce the footprint of the beamforming network. Moreover, in the millimeter-wave frequency range the transmission technologies are decisive since they impose the level of propagation losses. Microstrip or coplanar waveguides present a high loss level at high frequencies due to the substrate and radiation losses. Substrate Integrated Waveguide (SIW) is another planar technological solution for high frequency since it reduces the transmission loss level. A variety of SIW phase shifters in high frequency range have been presented [8]–[10]. In waveguide-based designs, stretching the broad side of the waveguide by utilizing metallic posts or etching air holes in the upper layer are the usual techniques used to introduce signal phase shift. However, for SIW technology, the presence of dielectric material imposes a strong efficiency drawback. Hollow waveguide technology is the most suitable technology in this frequency range. Nevertheless, metallic contact between waveguide plates is needed for avoiding unwanted signal leakage. Recently, gap waveguide technology has arisen to overcome waveguide plate contact and shielding requirements [11], [12]. Different phase shifters using gap waveguide technology are presented in [13]–[15]. Dielectric material use and low compactness are the principal disadvantages in these designs. On the other hand, there are waveguide-based phase shifter solutions that have a good performance in millimeter-wave range but they are highly complex and have a high manufacturing cost [16], [17].

Metasurfaces can also provide signal phase shift. Tuning the design of the metasurface, the phase shift can be controlled. One of the best advantage for this kind of phase shifter is that, for the same size, the phase shift can be different, depending on the design [18]. In these terms, a recent study [19] presents a prototype made in groove gap waveguide technology that uses a pin lattice to get the desired phase shift. Compared to other previous designs that make use of corrugated ridges [20], it is demonstrated that a higher phase shift and a higher compactness can be achieved by using pin lattices.

Structures with higher symmetries make possible to tailor the signal propagation behavior [21]. Some intensive studies about structures that posses higher symmetries have been recently presented [22]–[24]. Based on higher symmetries, it is possible to widen stop-bands or to control the equivalent refractive index. Some examples such as lenses or filters in microwave and millimeter-wave range based on higher symmetries are [25] and [26]. Thus, introducing higher symmetries in electromagnetic devices permits a new degree of freedom in the design process.

This work presents a waveguide phase shifter working in millimeter-wave and based on higher symmetries. Glide symmetry is the chosen type of higher symmetry to achieve a greater phase shift for the same waveguide length. A unit cell has glide symmetry configuration if it is generated by a translation of half unit cell period and a mirroring regarding to a symmetry plane [21].

The document is organized as follows: Section I introduces the phase shifter designs for the millimeter-wave range. In Section II, the phase shifting unitary cells are presented and studied by means of the dispersion diagrams. Section III provides the description and design of the glide-symmetric phase shifter, joined to its comparison with the non-glide-symmetric counterpart. Section IV introduces the manufactured prototype and presents the measurement results. Finally, the conclusions are drawn in section V.

II. GLIDE-SYMMETRIC PIN STRUCTURES

Glide symmetry is the most suitable higher symmetry for this kind of phase shifter structures. Through the application of glide symmetry to the pin lattice that composes the phase shifter, the electromagnetic performance can be significantly improved and controlled. In this section, the forming phase shifting unitary cells for the different configurations are presented and analyzed through dispersion diagram studies.

A. PHASE SHIFTING UNITARY CELLS

Phase shifter based on a cascade of pin rows located perpendicular to the propagation direction can be divided into unitary phase shifting cells, as it is illustrated in Figure 1. Two types of unitary cells are depicted in 3D, longitudinal and

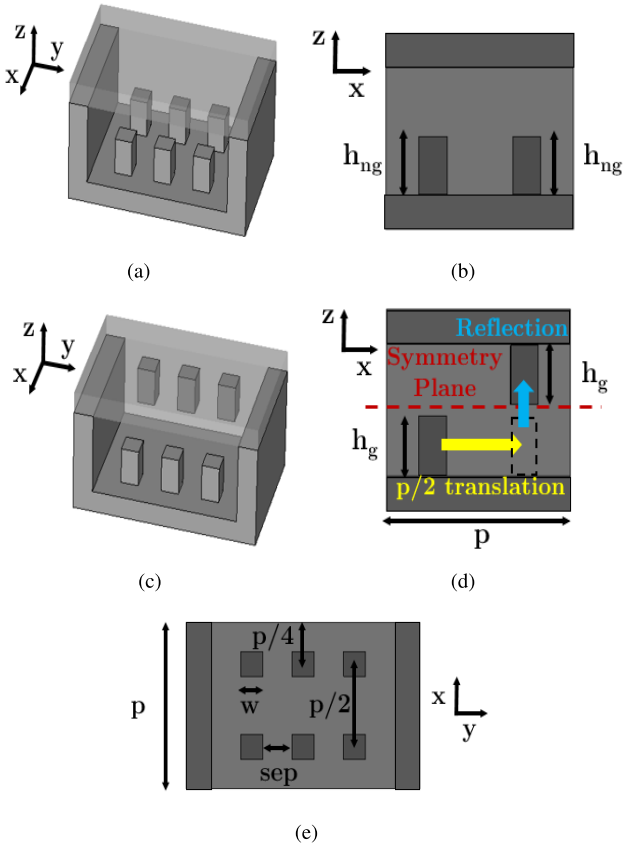

FIGURE 1. Phase shifting unitary cells: (a) non-glide-symmetric design, (b) its longitudinal cutting view, (c) glide-symmetric design, (d) its longitudinal cutting view, and (e) top view.

top view. The non-glide-symmetric unitary cell (Figure 1(a)) corresponds to the unitary cell that forms the phase shifter state-of-art presented in [19].

The metallic pins that compose the phase shifter are placed only in one broad side of the waveguide. Glide symmetry is applied to each pair of pin rows that form the non-glide-symmetric cell, taking advantage of having free the upper broad side of the waveguide. This pin row displacement to impose a glide-symmetric configuration in the unitary cell is depicted in Figure 1(d). The reference symmetry plane for pin mirroring is located in the middle of the lateral waveguide side and perpendicular to it. Note that, in the pin displacement, the heights of the pins (H) are preserved, which means that $H_{ng} = H_g$.

The top view illustrated in Figure 1(e) is the same for both phase shifting unitary cells. Considering p as the fixed unitary cell length, the distance between pin rows is $p/2$. The separation between pins in the transversal direction is denoted as sep. The width (W) and height (H) of the pins are also the other geometric variables that have influence in the performance of the phase shifter.

The following subsection shows the comparison between both phase shifting unitary cells, glide and non-glide, presented by means of their dispersion diagrams.

B. PERFORMANCE AND DISPERSION DIAGRAM COMPARISON

Dispersion diagrams let accurately demonstrate the performance of a guiding structure through the study of the propagating modes and their distribution in frequency. The position of the first propagating mode is normally the one that defines the working range and the forward mode dispersion properties. The dispersion diagrams contained in this study have been carried out with the eigenmode solver of *CST Microwave Studio*. Each dispersion diagram shows the first propagating mode of the unitary cell for a parametric sweep. Figure 2 and Figure 3 illustrate the dispersion diagram comparison between both types of unitary cell, including height and width pin tuning, respectively. The reference line corresponds to the first propagating mode of the WR-15 standard waveguide. The sweeps of pin heights and pin

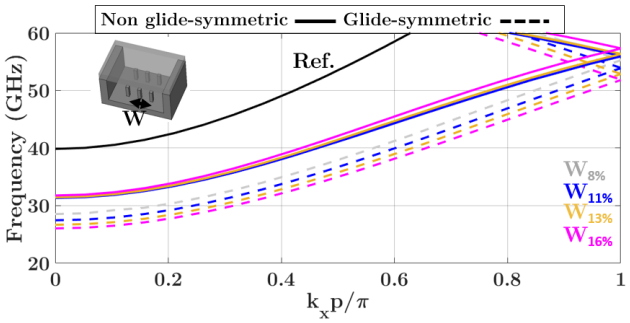

FIGURE 3. Dispersion diagram comparison modifying pin width. Dimensions are: $p = 2.1$ mm, $sep = 0.6$ mm and $H_{ng} = H_g = 0.85$ mm.

widths are referred, in percentage, to the narrow and broad waveguide side dimensions, respectively.

The height variation in the phase shifter pins have a higher influence in the dispersion behavior than the pin width variation. Both pin configurations, non-glide-symmetric and glide-symmetric, lower the first propagating mode regarding to the reference mode. This means that, for a given frequency, the propagation constant is increased. It can be identified that the glide-symmetric phase shifting unitary cell produces a higher propagation constant for any value of pin height and width than the non-glide case. This is directly translated into a higher phase shifting for the same waveguide length in the case of the glide-symmetric configuration. Therefore, the glide-symmetric unitary cell has a better performance in terms of phase shifting capacity compared to any other configuration. A remarkable propagation effect that appears in the mode distribution is the position of the initial propagation frequencies. The reference waveguide mode starts to propagate at approximately 40 GHz while the phase shifting unitary cell starts at 30 GHz in the case of $H_{45\%}$. This decrease in the cutoff frequency for the same waveguide size is useful for miniaturization and size reduction. This will be matter for further work since is not the scope of this document. Additionally, modifications in cell length (p) have been studied and illustrated in a dispersion diagram comparison in Figure 4. The normalization of the length, p, has been removed for a more realistic representation of the dispersion diagram and fair comparison between modes and their propagating properties.

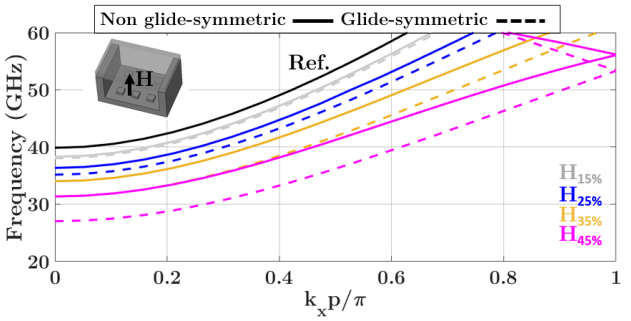

FIGURE 2. Dispersion diagram comparison modifying pin height. Dimensions are: $p = 2.1$ mm, $w = 0.45$ mm, $sep = 0.6$ mm and $H_{ng} = H_g$.

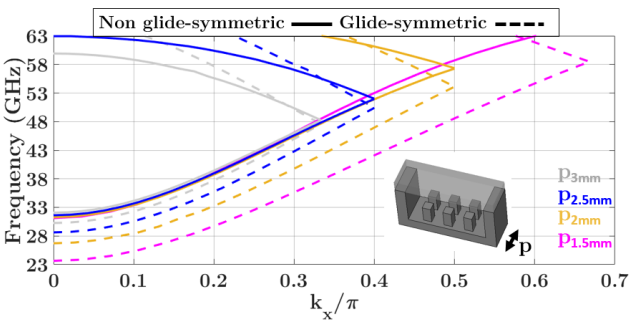

FIGURE 4. Dispersion diagram comparison modifying the cell length (p). Dimensions are: $W = 0.45$mm, $sep = 0.6$ mm and $H_{ng} = H_g = 0.85$ mm.

TABLE 1. Dimensions of both phase shifters [mm].

Parameters	w	p	h_1	h_2	h_3	h_4
Values	0.45	2.1	0.35	0.5	0.75	0.85

From these results, two main conclusions can be drawn. First, the length of the phase shifting unit cell does not affect the locations of the modes for the non-glide-symmetric unitary cell. However, for glide-symmetric unit cell, the frequency position of the modes decreases as the cell length is reduced. Second, the position of the cutting frequency between the two types of cell configuration is different. It is also noticed that, for greater values of p in the glide configuration, the cutting frequency between modes is reduced. This effect is due to the reduction of electromagnetic coupling between pin rows placed in in the glide-symmetric configuration. Therefore, the length of the unitary cell strongly affects the mode distribution and has to be carefully chosen for a proper effect of the glide symmetry in the frequencies of interest.

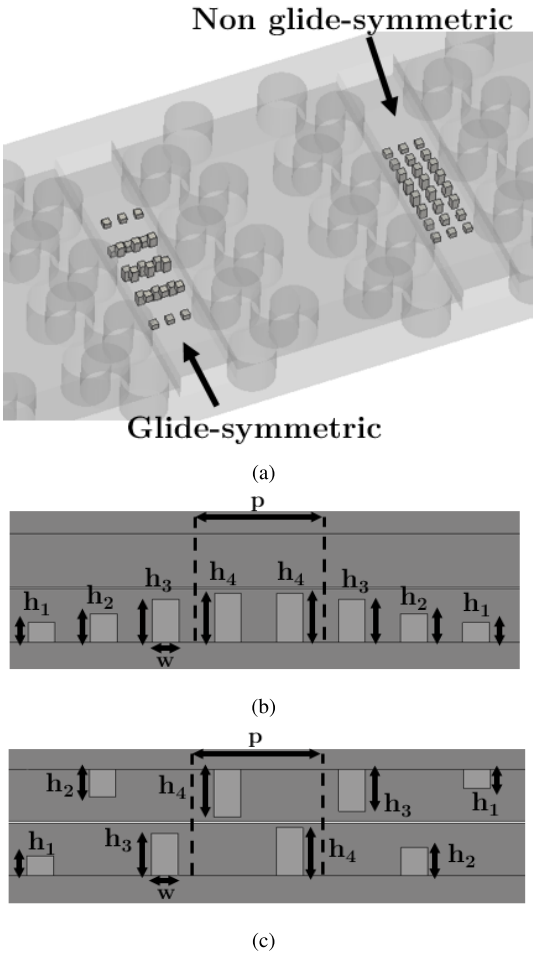

FIGURE 5. Phase shifter designs: (a) pin configurations integrated into the glide-symmetric holey gap waveguide, (b) longitudinal cutting view of the non-glide-symmetric configuration, (c) longitudinal cutting view of the glide-symmetric configuration. Transversal separation *sep* = 0.6 mm.

III. PHASE SHIFTER PERFORMANCE

The design of a complete phase shifter consists of several phase shifting unitary cell in cascade along the direction of propagation. The pin heights and cell length have to be properly chosen according to the phase delay required and the working frequency band. In this section, 53 GHz is fixed as the central frequency, providing a phase shift of 180 degrees for the glide configuration. Once the glide-symmetric phase shifter is designed complying with this requirement, the same pins are considered, but placed in non-glide-symmetric configuration. Figure 5 illustrates both phase shifter designs, non-glide-symmetric and glide-symmetric configurations, and the parameter values of each constituting unitary cell introduced. For a proper impedance matching, incremental tailoring of the pin row heights at both ends of the phase shifter are needed.

The gap waveguide technology employed for manufacturing both phase shifters and a reference waveguide, is the glide-symmetric holey gap waveguide reported in [27] and [28]. This technology provides very low manufacturing costs with a great waveguide propagation performance. The periodic glide-symmetric holey structure used provides a stop band from 36 to 70 GHz. The holey-glide-symmetric unit cell posses these dimensions: hole diameter $2r = 3.5$ mm, hole depth $h = 3.6$ mm, unit cell size $a = 5.36$ mm and gap $g = 0.05$ mm. Complete information regarding this manufacturing technology and design guidelines can be found in the referred work [28].

A. DESIGN AND SIMULATION RESULTS

In order to validate these results, a complete prototype is designed, shown in Figure 6. It is formed by three WR-15 gap

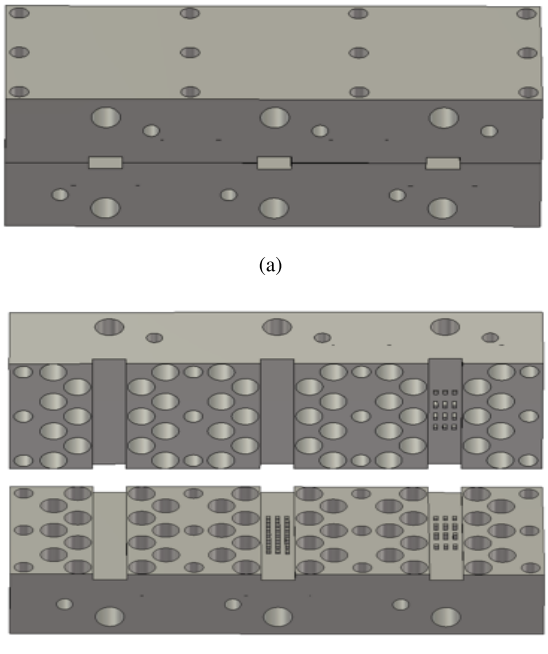

FIGURE 6. Phase shifter prototype design: (a) assembled (b) upper and lower parts.

waveguide, each one with a different configuration: reference waveguide (without pins), non-glide-symmetric phase shifter and glide-symmetric phase shifter. Glide-symmetric holes are included in both sides of each waveguide path for avoiding signal leakage and coupling.

The simulation results are illustrated in Figure 7. Both phase shifters achieve a great bandwidth, from 46 to 60 GHz with insertion losses below 0.5 dB.

Regarding to the phase behavior, both phase shifters have a higher phase shift than the reference waveguide. The glide-symmetric phase shifter provides a greater phase shift along the whole frequency band. Nevertheless, this difference in phase decreases as frequency increases.

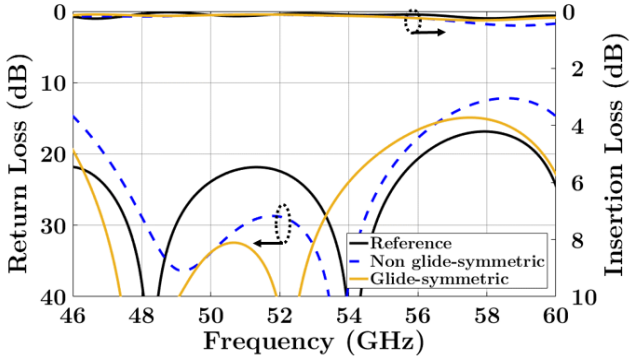

(a)

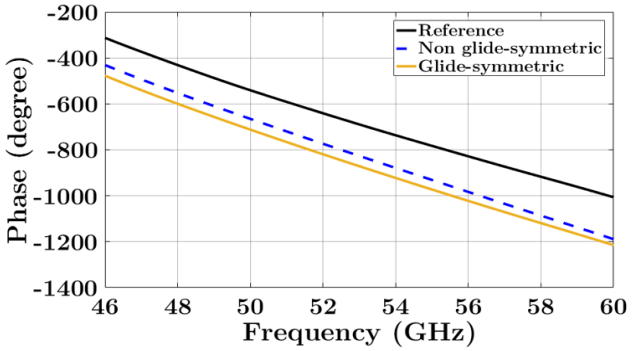

(b)

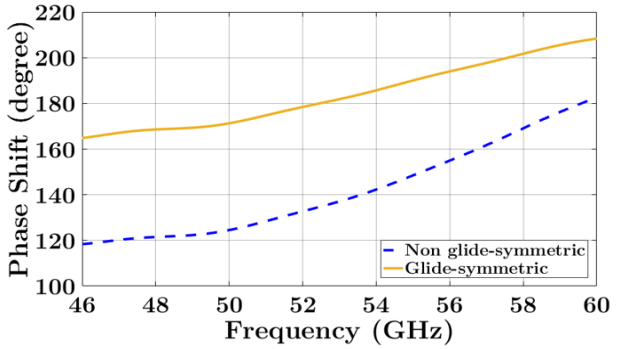

(c)

FIGURE 7. Simulated S-Parameters of the phase shifters and reference waveguide. (a) Return loss and insertion loss. (b) Unwrapped phase of S_{21}. (c) Phase shift referred to the reference waveguide.

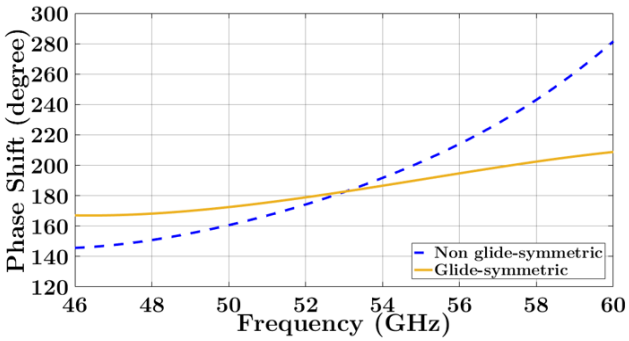

FIGURE 8. Phase shift referred to the reference waveguide when non-glide-symmetric is designed to produce 180 degrees at 53 GHz.

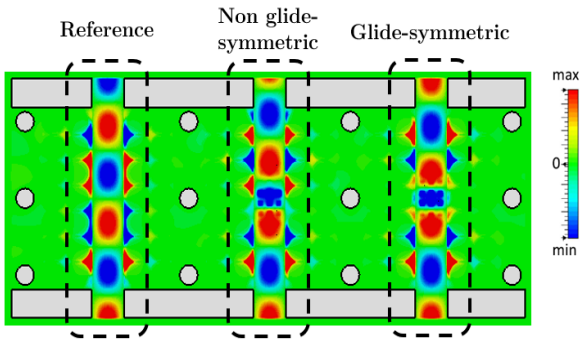

FIGURE 9. E-field distribution for the phase shifters and the reference waveguide at 53 GHz.

Figure 7(c) illustrates the phase shift produced by each phase shifter regarding the reference waveguide phase. It is noticed that, at the center frequency, the phase shift provided by the glide-symmetric phase shifter is 40 degrees higher than its non-glide-symmetric version. This difference in phase shift was predicted in the previous dispersion diagram study. Moreover, the difference between both phase shift graphs decreases as frequency increases since they are approaching to the cutting frequency between modes.

Additionally, non-glide-symmetric phase shifter can be designed to produce 180 degrees phase shift by means of enlarging the pins. However, its phase deviation with the same reference phase degree (180 degrees at 53 GHz) is bigger than the glide-symmetric phase shifter case as Figure 8 shows. This higher phase deviation in the non glide-symmetric case can be explained through linearity comparison in Figure 4. The glide-symmetric case provides a less dispersive propagating mode than the non-glide-symmetric case when the frequency increases. Table 2 shows the performance differences between both depicted phase shifter designs. Also, some aspects about manufacturing are listed.

TABLE 2. Comparison between non-glide-symmetric and glide-symmetric phase shifter designs.

Phase Shifter design	Compactness (degree/mm) (Simulated Results)	Phase deviation (degree) regarding to Figure 8	Manufacturing
Non glide-symmetric	16.7	±65	Hard due to large and close pins
Glide-symmetric	22.1	±20	Easy due to small pins and bigger separation between pins

TABLE 3. Comparison between proposed and reported waveguide phase shifters.

Ref.	Frequency (GHz)	Compactness (degree/mm)	Complexity	Use of Dielectric	Insertion Loss (dB)
[15]	44.5-61	7.56	Low	Yes	<1.5
[8]	26.5-40	4.63	Low	Yes	<0.4
[16]	85-115	7.08	High	No	<0.2
[17]	33-50	11.49	High	No	<9
This work	46-60	25	Low	No	<1

Gap waveguide technology confines the propagation signal inside waveguides and avoids any coupling between paths. A clear vision of this fact and the difference between the field distribution for both phase shifters is illustrated in Figure 9, where the absolute E-field distribution in the gap plane is presented.

IV. PROTOTYPE MEASUREMENTS

Once designed, the prototype has been manufactured to validate the simulation results discussed above. For manufacturing, the technique used is CNC milling. The prototype is presented in Figure 10. Some screws are introduced between each row of glide-symmetric holes to achieve an accurate assembly.

FIGURE 10. CNC milling manufactured prototype.

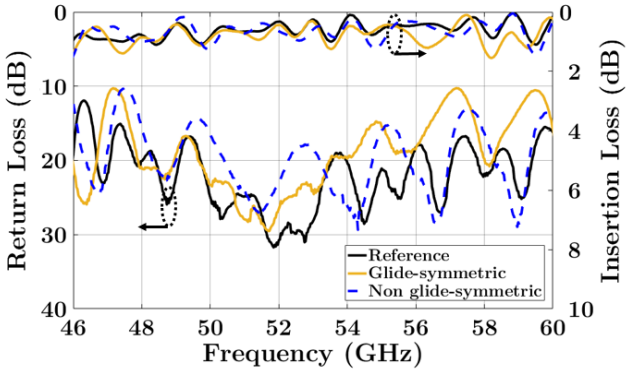

(a)

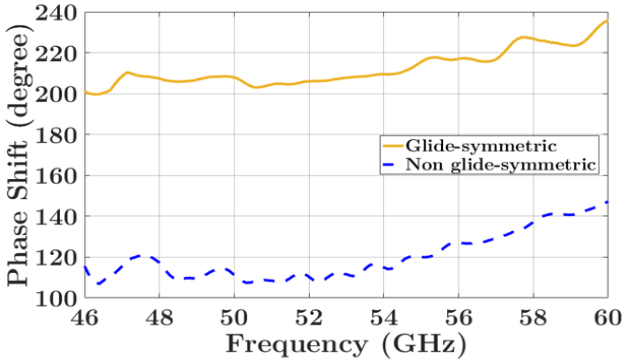

(b)

FIGURE 11. Measured S-Parameters of the phase shifters and the reference waveguide. (a) Return loss and insertion loss. (b) Phase shift referred to the reference waveguide.

The prototype has been measured from 46 to 60 GHz with a R&S-ZVA67 VNA and the results are depicted in Figure 11(a). Regarding to the S-parameters, the return loss is higher than 10 dB in the whole frequency band for both phase shifters. On the other hand, the insertion loss of both phase shifters are very similar. The maximum is 1 dB of losses in the entire operational band. The slight increase of 0.5 dB of insertion losses compared to simulations are due to the manufacturing process, and are negligible for the phase behavior validation. Also, the ripple presented in all of the measured S-parameters are caused by the use of 1.85mm coaxial to WR-15 waveguide transitions in the measurement process. Nevertheless, there is an appropriate agreement between simulations and measurements. The comparison between the

measured phase shift achieved for each phase shifter is illustrated in the Figure 11(b). It is observed a difference in phase shift between the glide-symmetric and non-glide-symmetric pin configurations quite similar to the simulation results. The phase shift difference between both phase shifters is around 80 degrees. The phase shift provided by the glide-symmetric phase shifter is 40 degrees greater than the simulation results. The reason of this increment could be related to a higher height in the pins during the manufacturing process. Therefore, taking in to account the length of the phase shifter, a compactness of 25 degrees per millimeter can be achieved in comparison with the 15 degrees per millimeter provided by the non-glide-symmetric configuration. The table 3 presents a comparison with others reported works. This work presents a phase shifter design in a fully metallic structure with high compactness and low loss. Additionally, the phase shifter with the glide-symmetric pin configuration has an advantage in the pin manufacturing. The pins that compose the phase shifter are easier to manufacture since the distance between pins can be greater to achieve equal phase shift than in the non-glide-symmetric version.

V. CONCLUSIONS

In this work, we have presented a compact and low-loss V-band waveguide phase shifter design technique based on glide-symmetric pin configuration. This kind of higher symmetry permits the control and improvement of the electromagnetic behavior or radiofrequency devices. It has been demonstrated that the pin configuration is the proper option for introducing higher phase shifting effect in a waveguide-based system. There is significant increase in terms of phase shift when using a glide-symmetric pin distribution compared to its corresponding non-glide-symmetric configuration. A prototype has been manufactured in order to validate the theoretical approach through the comparison of phased shifters with both non-glide-symmetric and glide-symmetric configurations. The measurement results demonstrate the higher performance and compactness of the glide-symmetric phase shifter. For the same distance, the glide-symmetric version of the phase shifter provides more than 60% of phase shifting compared to the non-glide-symmetric phase shifter. Both phase shifters have proper impedance matching between 46 to 60 GHz and insertion loss levels lower than 1 dB in the entire band.

REFERENCES

[1] W. Hong *et al.*, "Multibeam antenna technologies for 5G wireless communications," *IEEE Trans. Antennas Propag.*, vol. 65, no. 12, pp. 6231–6249, Dec. 2017.

[2] T. Djerafi, N. Fonseca, and K. Wu, "Broadband substrate integrated waveguide 4×4 nolen matrix based on coupler delay compensation," *IEEE Trans. Microw. Theory Techn.*, vol. 59, no. 7, pp. 1740–1745, Aug. 2011.

[3] A. Tamayo-Dominguez, J. Fernandez-Gonzalez, and M. S. Castaner, "Low-cost millimeter-wave antenna with simultaneous sum and difference patterns for 5G point-to-point communications," *IEEE Commun. Mag.*, vol. 56, no. 7, pp. 28–34, Jul. 2018.

[4] J.-W. Lian, Y.-L. Ban, Q.-L. Yang, B. Fu, Z.-F. Yu, and L.-K. Sun, "Planar millimeter-wave 2-D beam-scanning multibeam array antenna fed by compact SIW beam-forming network," *IEEE Trans. Antennas Propag.*, vol. 66, no. 3, pp. 1299–1310, Mar. 2018.

[5] J.-W. Lian, Y.-L. Ban, C. Xiao, and Z.-F. Yu, "Compact Substrate-Integrated 4×8 butler matrix with sidelobe suppression for millimeter-wave multibeam application," *IEEE Antennas Wireless Propag. Lett.*, vol. 17, no. 5, pp. 928–932, May 2018.

[6] K. Tekkouk, J. Hirokawa, R. Sauleau, M. Ettorre, M. Sano, and M. Ando, "Dual-layer ridged waveguide slot array fed by a butler matrix with sidelobe control in the 60-GHz band," *IEEE Trans. Antennas Propag.*, vol. 63, no. 9, pp. 3857–3867, Sep. 2015.

[7] Q.-L. Yang, Y.-L. Ban, J.-W. Lian, Z.-F. Yu, and B. Wu, "SIW butler matrix with modified hybrid coupler for slot antenna array," *IEEE Access*, vol. 4, pp. 9561–9569, 2016.

[8] F. Parment, A. Ghiotto, T. P. Vuong, J. M. Duchamp, and K. Wu, "Double dielectric slab-loaded air-filled SIW phase shifters for high-performance millimeter-wave integration," *IEEE Trans. Microw. Theory Techn.*, vol. 64, no. 9, pp. 2833–2842, Sep. 2016.

[9] T. Yang, M. Ettorre, and R. Sauleau, "Novel phase shifter design based on substrate-integrated-waveguide technology," *IEEE Microw. Wireless Compon. Lett.*, vol. 22, no. 10, pp. 518–520, Oct. 2012.

[10] I. Boudreau, K. Wu, and D. Deslandes, "Broadband phase shifter using air holes in substrate integrated waveguide," in *IEEE MTT-S Int. Microw. Symp. Dig.*, Baltimore, MD, USA, Jun. 2011, pp. 1–4.

[11] P.-S. Kildal, A. U. Zaman, E. Rajo-Iglesias, E. Alfonso, and A. Valero-Nogueira, "Design and experimental verification of ridge gap waveguide in bed of nails for parallel-plate mode suppression," *IET Microw., Antennas Propag.*, vol. 5, no. 3, pp. 262–270, Feb. 2011.

[12] H. Raza, J. Yang, P.-S. Kildal, and E. Alfonso, "Resemblance between gap waveguides and hollow waveguides," *IET Microw., Antennas Propag.*, vol. 7, no. 15, pp. 1221–1227, Dec. 2013.

[13] A. Algaba-Brazalez and E. Rajo-Iglesias, "Design of a butler matrix at 60 GHz in inverted microstrip gap waveguide technology," in *Proc. IEEE Int. Symp. Antennas Propag. USNC/URSI Nat. Radio Sci. Meeting*, Vancouver, BC, Canada, Jul. 2015, pp. 2125–2126.

[14] M. A. Abdelaal, S. I. Shams, and A. A. Kishk, "Compact RGW differential phase shifter for millimeter-wave applications," in *Proc. 18th Int. Symp. Antenna Technol. Appl. Electromagn. (ANTEM)*, Waterloo, ON, Canada, Aug. 2018, pp. 1–2.

[15] E. Rajo-Iglesias, M. Ebrahimpouri, and O. Quevedo-Teruel, "Wideband phase shifter in groove gap waveguide technology implemented with glide-symmetric holey EBG," *IEEE Microw. Wireless Compon. Lett.*, vol. 28, no. 6, pp. 476–478, Jun. 2018.

[16] M.-H. Chung, D.-H. Je, S.-T. Han, and S.-R. Kim, "Development of a 85Φ115 GHz 90-deg phase shifter using corrugated square waveguide," in *Proc. 44th Eur. Microw. Conf.*, Oct. 2014, pp. 1146–1149.

[17] E. Villa, B. Aja, J. Cagigas, E. Artal, and L. de la Fuente, "Four-state full Q-band phase shifter using smooth-ridged waveguides," *IEEE Microw. Wireless Compon. Lett.*, vol. 27, no. 11, pp. 995–997, Nov. 2017.

[18] Z. Qamar, S. Y. Zheng, W. S. Chan, and D. Ho, "An equal-length multi-way differential metamaterial phase shifter," *IEEE Trans. Microw. Theory Techn.*, vol. 65, no. 1, pp. 136–146, Jan. 2017.

[19] S. A. Razavi and A. U. Zaman, "A compact phase shifter in groove gap waveguide for millimeter-wave applications," in *Proc. 12th Eur. Conf. Antennas Propag. (EuCAP)*, London, U.K., 2018, pp. 212–213.

[20] A. Tribak, Á. M. Sánchez, J. Zbitou, and J. L. Cano, "Novel ridged waveguide differential phase shifter for satellite application," *Int. J. Microw. Opt. Technol.*, vol. 9, no. 6, pp. 409–414, Nov. 2014.

[21] A. Hessel, M. H. Chen, R. C. M. Li, and A. A. Oliner, "Propagation in periodically loaded waveguides with higher symmetries," *Proc. IEEE*, vol. 61, no. 2, pp. 183–195, Feb. 1973.

[22] G. Valerio, F. Ghasemifard, Z. Sipus, and O. Quevedo-Teruel, "Glide-symmetric all-metal holey metasurfaces for low-dispersive artificial materials: Modeling and properties," *IEEE Trans. Microw. Theory Techn.*, vol. 66, no. 7, pp. 3210–3223, Jul. 2018.

[23] O. Dahlberg, R. Mitchell-Thomas, and O. Quevedo-Teruel, "Reducing the dispersion of periodic structures with twist and polar glide symmetries," *Sci. Rep.*, vol. 7, Aug. 2017, Art. no. 10136 .

[24] F. Ghasemifard, M. Norgren, O. Quevedo-Teruel, and G. Valerio, "Analyzing glide-symmetric holey metasurfaces using a generalized floquet theorem," *IEEE Access*, vol. 6, pp. 71743–71750, 2018.

[25] P. Padilla, L. F. Herrán, A. Tamayo-Domínguez, J. F. Valenzuela-Valdés, and O. Quevedo-Teruel, "Glide symmetry to prevent the lowest stopband of printed corrugated transmission lines," *IEEE Microw. Wireless Compon. Lett.*, vol. 28, no. 9, pp. 750–752, Sep. 2018.
[26] O. Quevedo-Teruel, J. Miao, M. Mattsson, A. Algaba-Brazalez, M. Johansson, and L. Manholm, "Glide-symmetric fully metallic luneburg lens for 5G communications at ka-band," *IEEE Antennas Wireless Propag. Lett.*, vol. 17, no. 9, pp. 1588–1592, Sep. 2018.
[27] M. Ebrahimpouri, E. Rajo-Iglesias, Z. Sipus, and O. Quevedo-Teruel, "Cost-effective gap waveguide technology based on glide-symmetric holey EBG structures," *IEEE Trans. Microw. Theory Techn.*, vol. 66, no. 2, pp. 927–934, Feb. 2018.
[28] M. Ebrahimpouri, O. Quevedo-Teruel, and E. Rajo-Iglesias, "Design guidelines for gap waveguide technology based on glide-symmetric holey structures," *IEEE Microw. Wireless Compon. Lett.*, vol. 27, no. 6, pp. 542–544, Jun. 2017.

ANGEL PALOMARES-CABALLERO was born in Jaén, Spain, in 1994. He received the B.Sc. and M.Sc. degrees in telecommunication engineering from the University of Granada, Spain, in 2016 and 2018, respectively, where he is currently pursuing the Ph.D. degree with the Department of Signal Theory, Telematics and Communications. In 2018, he joined the Department of Language and Computer Science, Universidad de Málaga. His research interests include millimeter-wave antennas, gap waveguide, optimization algorithms, and structures with higher symmetries.

ANTONIO ALEX-AMOR received the B.Sc. degree in telecommunication engineering from the Universidad de Granada, in 2016, and the M.Sc. degree in telecommunication engineering from the Universidad Politécnica de Madrid (UPM), in 2018, where he is currently pursuing the Ph.D. degree. Since 2016, he has been with the Radiation Group, Signal, Systems and Radiocommunications Department, UPM, and in 2018, he joined the Department of Language and Computer Science, Universidad de Málaga. His current research interests include the use of liquid crystal as tunable dielectric, radiofrequency energy harvesting systems, and higher symmetry structures.

PABLO PADILLA was born in Jaén, Spain, in 1982. He received the Telecommunication Engineering degree and the Ph.D. degree from the Radiation Group, Signal, Systems and Radiocommunications Department, Technical University of Madrid (UPM), Spain, in 2005 and 2009, respectively. In 2007, he was with the Laboratory of Electromagnetics and Acoustics, École Polytechnique Fédérale de Lausanne, Switzerland, as an invited Ph.D. Student. In 2009, he carried out a Postdoctoral stay at the Helsinki University of Technology (AALTO-TKK), and in 2009, he was an Assistant Professor with the Signal Theory, Telematics and Communications Department, University of Granada, where he has been an Associate Professor, since 2012. In 2017, he was a Visiting Professor with the Royal Institute of Technology of Stockholm. He has authored more than 60 high-impact journal contributions and more than 50 contributions to international symposia. His research interests include a variety area of knowledge related mainly to electromagnetism and communication topics (radiofrequency devices, antennas, and propagation).

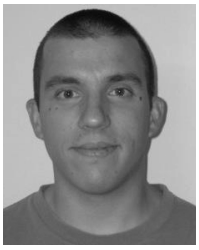

FRANCISCO LUNA received the degree in engineering and the Ph.D. degree in computer science from the University of Málaga, Spain, in 2002 and 2008, respectively, where he was a Research Assistant until 2012. In 2012, he joined the Universidad Carlos III of Madrid with a postdoctoral position, and in 2013, the Universidad de Extremadura as an Assistant Professor. Since 2015, he has been an Associate Professor with the University of Málaga. His current research interests include the design and implementation of parallel and multi-objective meta-heuristics, and their application to solve complex problems arising in several domains, including telecommunications, finance, and structural design.

JUAN VALENZUELA-VALDES was born in Marbella, Spain. He received the degree in telecommunications engineering from the Universidad de Malaga, Spain, in 2003, and the Ph.D. degree from the Universidad Politécnica de Cartagena, Spain, in 2008, where he joined the Department of Information Technologies and Communications, in 2004. In 2007, he joined EMITE Ing. as the Head of research. In 2011, he joined the Universidad de Extremadura, and in 2015, he joined the Universidad de Granada, where he is currently an Associate Professor. His current research interests include wireless communications and efficiency in wireless sensor networks. He has also received several prizes, including a National Prize to the Best Ph.D. in Mobile Communications by Vodafone and the i-Patentes Award by the Spanish Autonomous Region of Murcia for innovation and technology transfer excellence. He is the Co-Founder of Emite Ing, a spin-off company. He also holds several national and international patents. His publication record comprised of more than 80 publications, including 40 JCR indexed articles, more than 30 contributions in international conferences, and seven book chapters.